Acta Oceanol. Sin., 2018, Vol. 37, No. 9, P. 22–28
DOI: 10.1007/s13131-018-1262-9
http://www.hyxb.org.cn
E-mail: hyxbe@263.net

Relationship between a function of the northward pressure gradient and the Pacific Equatorial Undercurrent

CHEN Xuan[1, 2, 5], ZHENG Chongwei[2, 3, 4, 5], WU Hui[2], YOU Xiaobao[3, 5]*, LI Xunqiang[6], WANG Huipeng[1]

[1] The 75839 Army, People's Liberation Army, Guangzhou 510510, China

[2] State Key Laboratory of Estuarine and Coastal Research, East China Normal University, Shanghai 200062, China

[3] Institute of Atmospheric Physics, Chinese Academy of Sciences, Beijing 100029, China

[4] State Key Laboratory of Numerical Modeling for Atmospheric Sciences and Geophysical Fluid Dynamics, the Institute of Atmospheric Physics, Chinese Academy of Sciences, Beijing 100029, China

[5] Beijing Institute of Applied Meteorology, Beijing 100029, China

[6] College of Meteorology and Oceanography, National University of Defense Technology, Nanjing 211101, China

Received 11 March 2017; accepted 25 December 2017

Abstract

The Equatorial Undercurrent (EUC) plays an important role in ocean circulation and global climate change. Near the equator, as the Coriolis parameter goes to 0, equatorial currents cannot be described by geostrophy in which the pressure gradient force term is balanced by the Coriolis force term. Many previous studies focus on the relationships between the EUC and El Niño-Southern Oscillation (ENSO), the thermocline, sea surface topography, the distribution of equatorial wind stress and other atmosphere-ocean factors. However, little attention has been paid to the northward pressure gradient (NGT), which may also be important to the EUC. The pressure can be regarded as a complex nonlinear function of terms including temperature, salinity and density. This study attempts to reveal the connection between a function of the northward pressure gradient (FNP) and the EUC. The connection is derived from primitive equations, by simplifying the equations with using scaling analysis, and shows that the beta effect may be the main reason why the FNP is important to the EUC. The vertical structure of the EUC can be partially described by the FNP. The NGT has an obvious influence on the EUC while the eastward pressure gradient has a relatively smaller effect.

Key words: Equatorial Undercurrent, northward pressure gradient, beta effect

Citation: Chen Xuan, Zheng Chongwei, Wu Hui, You Xiaobao, Li Xunqiang, Wang Huipeng. 2018. Relationship between a function of the northward pressure gradient and the Pacific Equatorial Undercurrent. Acta Oceanologica Sinica, 37(9): 22–28, doi: 10.1007/s13131-018-1262-9

1 Introduction

The Equatorial Undercurrent (EUC) is the last major oceanic current discovered by Cromwell, and is also known as Cromwell Current. Although easterly winds blow over the equator, the EUC is a strong and steady eastward flowing current and is closely related to the upper-ocean conditions (Wang and Müller, 2002; Wang et al., 1993, 2009), the Indian Ocean dipole (Swapna and Krishnan, 2008) and other atmosphere-ocean phenomena (Yu and Mcphaden, 1999; Kessler, 2006; Constantin and Johnson, 2015; Holmes and Thomas, 2015; Zheng and Li, 2017; Zheng et al., 2018a, b). However, there is no complete theory for understanding the EUC. With the development of observational technology and numerical simulations, increasing amounts of data are available for research into the EUC (Brandt et al., 2014; Drenkard and Karnauskas, 2014; Izumo, 2005; Johns et al., 2014). The characteristics of the EUC are much clearer, but there is no diagnostic relation for the EUC, and it is still hard to explain the mechanism that drives the EUC. Crawford (1982), Pedlosky (1987), Pedlosky and Samelson (1989), Yin and Sarachik (1993) and many other researchers have focused on theoretical methods to explain the EUC, in terms of the β-effect or potential vorticity.

Another approach is to use numerical methods or models, such as oceanic general circulation models (OGCMs) (Qiu et al., 2013), large-eddy simulation models (Pham et al., 2013), ocean circulation and climate advanced model (OCCAM) (Hazeleger et al., 2003), and hybrid coordinate ocean model (HYCOM) (Wang et al., 2016). Most of these studies have focused on the temperature, eastward pressure gradient (EGT), relations with El Niño-Southern Oscillation (ENSO), sea surface height, and so on, but very few mentioned the NGT. The relationship between the function of the northward pressure gradient (FNP) and the EUC can be derived from the primitive equations; this relationship is in essence a balance between the pressure and the EUC. The relationship may explain part of the EUC as the FNP is also affected by the sea surface height, temperature and salinity.

Starting from the primitive equations, the relationship between the FNP and the EUC is derived in Section 2 and the diagnostic results based on the relationship are shown in Section 3.

Foundation item: The Open Research Fund of State Key Laboratory of Estuarine and Coastal Research of China, East China Normal University under contract No. SKLEC-KF201707; the National Natural Science Foundation of China under contract No. 41490642; the Natural Science Foundation of Shandong Province of China under contract No. ZR2016DL09.
*Corresponding author, E-mail: yxb@mail.iap.ac.cn

Conclusions and a discussion are provided in Section 4.

2 Relationship between the FNP and EUC

We consider that the EUC is given by nonlinear partial differential equations (the primitive equations):

$$u\frac{\partial u}{\partial x}+v\frac{\partial u}{\partial y}=-\frac{1}{\rho}\frac{\partial p}{\partial x}+fv+A_H\Delta u+A_Z\frac{\partial^2 u}{\partial z^2}, \tag{1}$$

$$u\frac{\partial v}{\partial x}+v\frac{\partial v}{\partial y}=-\frac{1}{\rho}\frac{\partial p}{\partial y}-fu+A_H\Delta v+A_Z\frac{\partial^2 v}{\partial z^2}, \tag{2}$$

$$\frac{\partial u}{\partial x}+\frac{\partial v}{\partial y}=0, \tag{3}$$

where ρ is the sea water density; p is the sea water pressure; f is the Coriolis parameter; A_Z is vertical eddy diffusivity; A_H is horizontal eddy diffusivity; u and v are the zonal and meridional components of the velocity vector; and Δ is the two-dimensional Laplacian.

As the Coriolis parameter becomes very small, going to 0 at the equator, $\beta\left(\frac{\partial f}{\partial y}\right)$ becomes large and reaches its maximum. Near the equator, $f\approx\beta y$ (Pedlosky, 1987; Pedlosky and Samelson, 1989; Yin and Sarachik, 1993). In many studies, such as the papers listed in the references, it is assumed, both for diagnosing potential vorticity and interpreting observations, that the zonal velocity and meridional derivatives are specified. Such assumptions simplify the equations and make the structure of the EUC clearer; however, they do not reveal the relationship between pressure and the EUC. But the pressure is a very important factor, it is an important force in the primitive equations and can be regarded as a response to the whole ocean environment. In this context it seems obvious that the EGT is the main cause of the EUC since the Coriolis force goes to 0 at the equator. However, this idea may be not correct.

In the primitive equations, at the equator, the terms containing f will be neglected. However, there is another important factor—β will be neglected with f. If we neglect this parameter or focus on the potential vorticity, the relationship between the pressure and the EUC may not be clear.

The hypotheses in this paper for the EUC are stated here: (1) the EUC is eastward-flowing, with weak meridional flow; (2) near the equator, as $f\to0$, $\beta\to$maximum: this means that the β-effect cannot be neglected; and (3) at the equator, there is large variability in the sea surface temperature (Stewart, 2008), so we cannot take the density as a constant.

These assumptions mean that although the Coriolis force goes to 0 at the equator, the β-effect (Hughes, 1981) cannot be neglected. The β-effect is very important for equatorial velocity diagnosis (Sudre and Morrow, 2008), and in the primitive equations, if the Coriolis force term was initially neglected, we cannot draw any conclusions about how the β-effect works in the EUC.

Differentiating Eqs (1) and (2) with respect to y, and substituting Eq. (3) into Eqs (1) and (2) gives:

$$v=\frac{-\frac{1}{\rho}\frac{\partial^2 p}{\partial x\partial y}+\frac{1}{\rho^2}\frac{\partial\rho}{\partial y}\frac{\partial p}{\partial x}-f\frac{\partial u}{\partial x}+A_H\Delta\frac{\partial u}{\partial y}+A_Z\frac{\partial^3 u}{\partial z^2\partial y}-u\frac{\partial^2 u}{\partial x\partial y}}{\frac{\partial^2 u}{\partial y^2}-\beta}, \tag{4}$$

$$\frac{\partial u}{\partial y}\frac{\partial v}{\partial x}+\left(\frac{\partial u}{\partial x}\right)^2-u\frac{\partial^2 u}{\partial x^2}-v\frac{\partial^2 u}{\partial x\partial y}=$$
$$-\frac{1}{\rho}\frac{\partial^2 p}{\partial y^2}+\frac{1}{\rho^2}\frac{\partial\rho}{\partial y}\frac{\partial p}{\partial y}-\beta u-f\frac{\partial u}{\partial y}-A_H\Delta\frac{\partial u}{\partial x}-A_Z\frac{\partial^3 u}{\partial z^2\partial x}. \tag{5}$$

Substituting Eq. (4) into Eq. (5), and as this is at the equator, we neglect the Coriolis parameter and high orders of differential and nonlinear terms with respect to y:

$$u=\frac{A_Z\beta\frac{\partial^5\frac{1}{\rho}\frac{\partial p}{\partial x}}{\partial y^2\partial z^2\partial x}+A_H\beta\frac{\partial^5\frac{1}{\rho}\frac{\partial p}{\partial x}}{\partial y^2\partial x^3}-\frac{\beta^2}{\rho}\frac{\partial^2 p}{\partial y^2}}{\beta^3+\beta\frac{\partial^4\frac{1}{\rho}\frac{\partial p}{\partial x}}{\partial y^2\partial x^2}}. \tag{6}$$

Equation (6) clearly shows that the EUC is related to the pressure. In Eq. (6), both the EGT and the NGT contribute to the EUC. After scaling, Eq. (6) can be simplified to

$$u\approx-\frac{1}{\rho\beta}\frac{\partial^2 p}{\partial y^2}, \tag{7}$$

to give the relationship between the FNP $\left(-\frac{1}{\rho\beta}\frac{\partial^2 p}{\partial y^2}\right)$ and the EUC. Throughout Eqs (1) to (7), the wind stress is not taken into consideration. In Eq. (7), there is no dependence on the EGT. Is that right? Back to Eq. (1), and taking the geostrophic approximation into consideration, anywhere except on the equator, the EGT contributes to v; as the latitude decreases, the EGT is balanced by wind stress and nonlinear and diffusion terms, which may make the EGT do less work on the EUC directly.

In the tropical deep ocean, the equation of state for sea water can be written as

$$\rho=\rho_0\left[1-\alpha\left(T-T_0\right)+\gamma\left(S-S_0\right)\right], \tag{8}$$

where ρ_0 is the sea water density at the reference temperature T_0 and the reference salinity S_0; α is the thermal expansion coefficient; and γ is the salinity coefficient. At T_0=20°C, α attains a value of 2.5×10^{-4} °C^{-1}, and γ is 8×10^{-4}. Differentiating Eq. (7) with respect to z:

$$\frac{\partial u}{\partial z}+u\frac{\partial q}{\partial z}=\frac{g}{\beta}\frac{\partial^2 q}{\partial y^2}+\frac{g}{\beta}\left(\frac{\partial q}{\partial y}\right)^2, \tag{9}$$

where g is the acceleration due to gravity; and q=lnρ. Substituting Eq. (8) into Eq. (9), the relationship between the FNP and the EUC can be translated into a relationship between the sea temperature, sea salinity and the EUC, which gives information on the effect of the thermocline on the EUC.

As some theories take the wind stress into consideration, the control equation Eq. (7) can be extended to

$$u+\frac{A_Z}{\beta}\frac{\partial^3 u}{\partial z^2\partial x}+\frac{A_H}{\beta}\frac{\partial^3 u}{\partial x^3}=-\frac{1}{\rho\beta}\frac{\partial^2 p}{\partial y^2}, \tag{10}$$

where the surface condition can be written in terms of the wind stress $\tau_x=\rho A_Z\frac{\partial u}{\partial z}$.

3 Numerical method and diagnostic results

In this section, using SODA (Carton and Giese, 2010; Drenkard and Karnauskas, 2014; Sun et al., 2004) data sets, a diagnostic experiment is setup for comparison. Because calculating u from Eq. (7) requires calculating the difference operator twice, the open boundary conditions (OBC) are more important in the experiment, in order to maintain accuracy in the numerical scheme. In Section 3.1, the numerical method is presented to show that useful OBCs can be found; and the diagnostic current velocity calculated from the temperature and density from the SODA and comparison result with the SODA currents are shown in Section 3.2.

3.1 *Numerical method*

The diagnostic program includes the OBCs, whose formulations are derived from Taylor's theorem (TT). Suppose $\phi \in C^n [a, b]$, that $\phi^{(n+1)}$ exists in $[a, b]$, and for $x_0 \in [a, b]$, $x_0 + \Delta \in [a, b]$, where ϕ is the model variable and (a, b) are the regional boundaries for the model. The OBCs can be written as

$$\left.\begin{aligned} \phi'_1 &= \frac{-3\phi_1 + 4\phi_2 - \phi_3}{2\Delta} \\ \phi'_n &= \frac{\phi_{n-2} - 4\phi_{n-1} + 3\phi_n}{2\Delta} \end{aligned}\right\}, \tag{11}$$

$$\left.\begin{aligned} \phi''_1 &= \frac{\phi_1 - \phi_2 - \phi_3 + \phi_4}{2\Delta^2} \\ \phi''_n &= \frac{\phi_{n-3} - \phi_{n-2} - \phi_{n-1} + \phi_n}{2\Delta^2} \end{aligned}\right\}, \tag{12}$$

where $\phi_1 = \phi(a)$; and $\phi_n = \phi(b)$. The formulations are simpler than other OBCs.

On the basis of Eqs (11) and (12), the numerical solutions of a 1-D advection equation $\left(\frac{\partial u}{\partial t} + u\frac{\partial u}{\partial x} = 0\right)$ were performed: one with sine wave forcing at the left boundary and starting from a zero initial condition (Fig. 1), another starting from a sine wave as the initial condition but without forcing (Fig. 2). The results are shown below:

The discrete equation in linear ocean currents diagnosis scheme is the Sylvester equation which is very useful in oceanic-atmospheric numerical technology. The OBCs can also be used in diagnosing currents (Chen et al., 2017) in the ocean (Fig. 3; in this experiment, the bottom layer is the vertical boundary, and the geographic bounding coordinates are 6.25°–30.25°S, 80.25°–97.75°E); the results show that useful OBCs can be found in this study.

3.2 *Diagnostic results and comparison*

In this section, we will compare the diagnostic results (u_d) with the SODA data (u_S) by calculating the correlation coefficient (CC, r) between them from Eq. (13):

$$r = \frac{1}{n}\sum_{i=1}^{n}\left(\frac{u_{d,\,i} - \bar{u}_d}{\sigma_d}\right)\left(\frac{u_{S,\,i} - \bar{u}_S}{\sigma_S}\right), \tag{13}$$

where the subscript i indicates the spatial grid index (or the temporal index for the set from January 1978 to December 2008) in the tropical Pacific Ocean (140°–180°E) from the surface to 300 m depth; σ is the standard deviation for the velocity by the same subscript. All calculation results have been tested for significance.

On the basis of the SODA data and Eq. (7), the EUC was calcu-

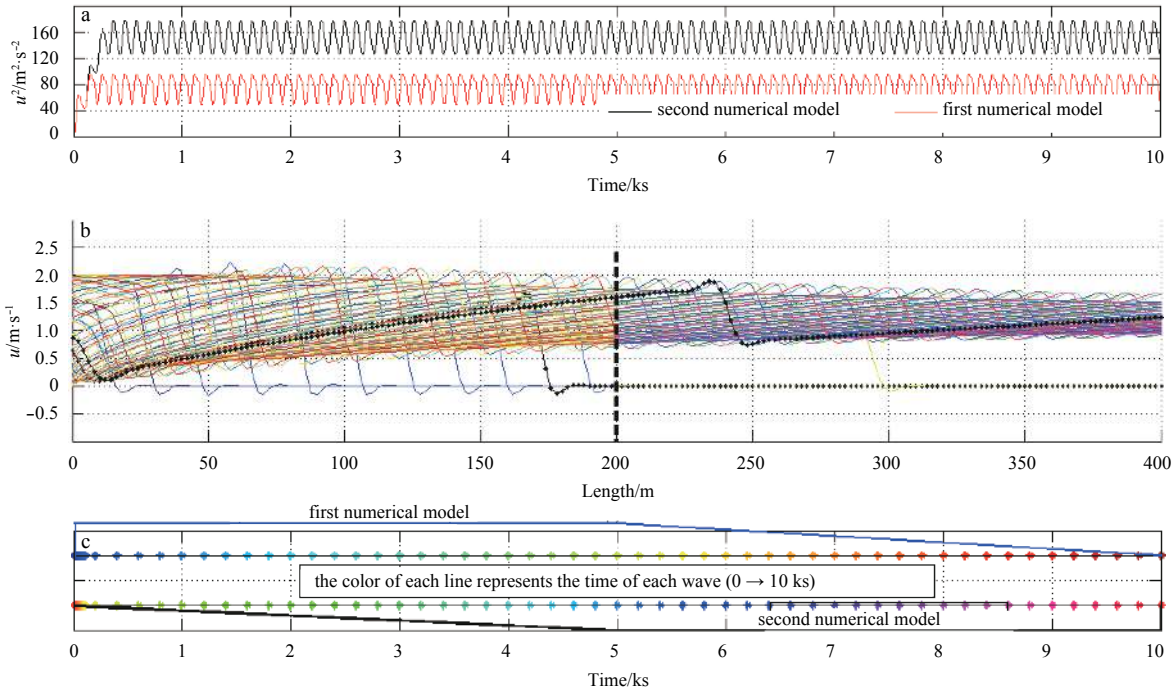

Fig. 1. The numerical results for the nonlinear 1-D advection equation. a. Time variation of the total energy, the black line is for the second numerical model, and the red line for the first numerical model; b. time evolution of the shape of the wave, the dashed line at 200 m is the boundary of the first model, but the middle of the second model. The color of each line represents the time of each wave as shown in the Fig. 1c, as the upper set of colors for the first model, and the lower set for the second model.

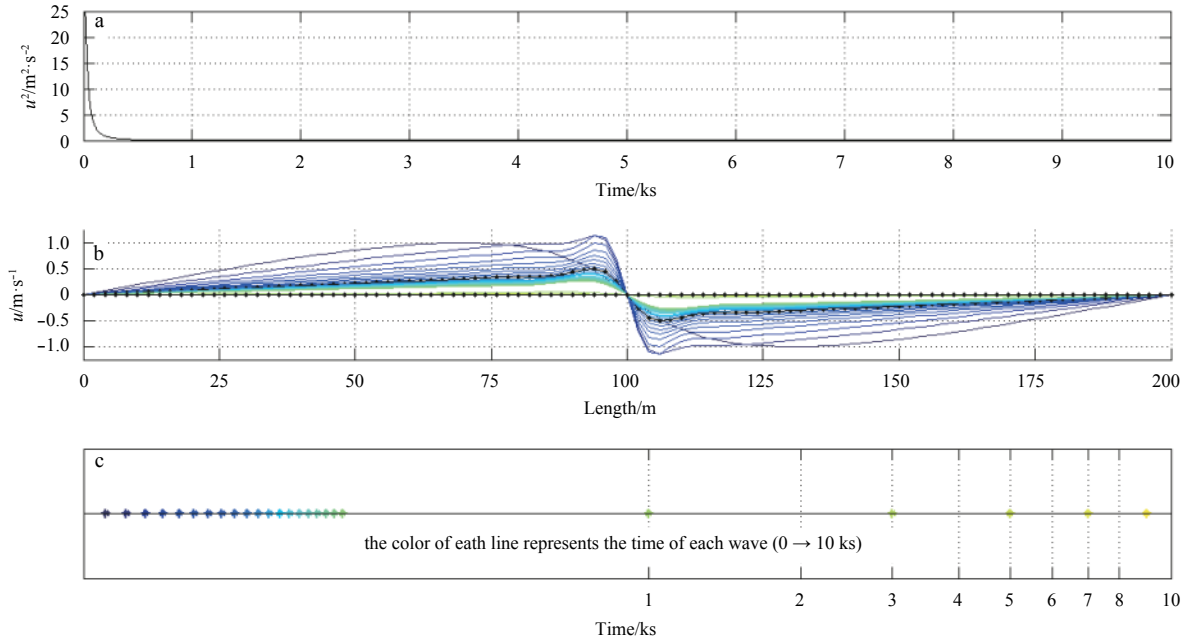

Fig. 2. The numerical results for the nonlinear 1-D advection equation. a. Time variation of the total energy, b. time evolution of the shape of the wave, and the color of each line represents the time of each wave as shown in Fig. 2c.

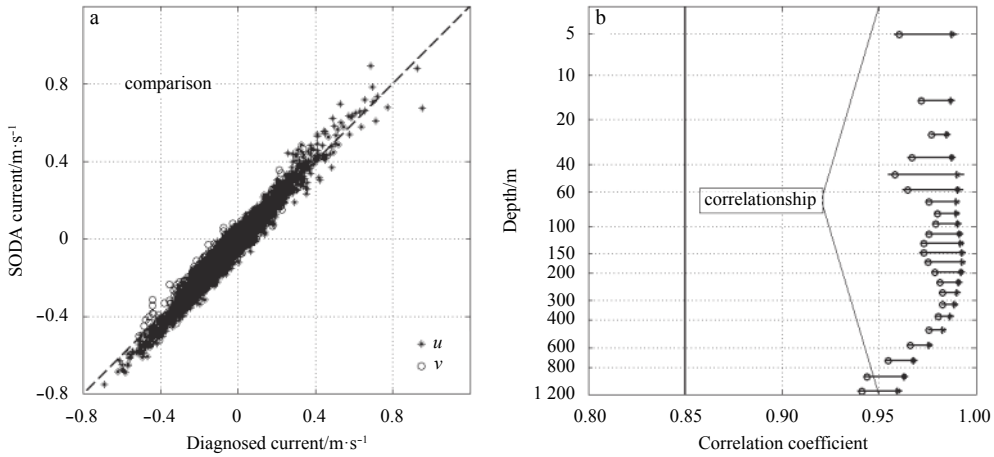

Fig. 3. The comparison between the diagnosed currents and SODA currents.

lated in this section. At first, taking these data sets (SODA_2.2.4_200001 and SODA_2.2.4_200007) as examples, the calculation area was the tropical Pacific Ocean. The diagnosed results of Eq. (7) are shown in Figs 4 and 5. All experiments include the data sets from January/1978 to December/2008 (Figs 6 and 7).

The CC between the FNP and the EUC in Figs 4 and 5 are about 0.881 3 and 0.832 5, respectively. Figures 4 and 5 show that the basic features of the EUC are retained in the diagnosed results: in Fig. 4, both the diagnosis and the SODA have two areas with eastward currents and three centers with maximum velocity in about the same position. Within the range of about 165°–172°E at a depth of about 150 m, both currents are westward. In Fig. 5, the velocities below 50 m are weak at 169°E in both diagnosis and SODA. In both cases, the diagnosed results retain the same basic features of the EUC as the SODA data sets.

The FNP is not independent of other processes; the pressure is a linear integral function of density, but the density is a complex nonlinear function of the pressure (or depth approximately), the sea temperature, and the salinity. So, we compared the EUC with the FNP, sea temperature, salinity, and the EGT, as all these factors are important in driving oceanic motion. In this study, we do not use output from any ocean models, such as HYCOM, so the influence of the wind stress on the EUC is difficult to evaluate as SODA only provides monthly wind stress data; the temporal resolution may be insufficient. The results of this comparison (the range of the SODA and the diagnostic results are same) in the experiments are shown in Fig. 6.

Figure 6 shows that the FNP is more closely associated with the EUC than are the temperature, the salinity, or the EGT. This result means that the EUC is a large-scale process; the β-effect is also important in this process. In some theories, the EUC may be driven by the EGT as a consequence of the sea surface topography being higher in the west of the Pacific Ocean, which causes the EGT along the equator. From Eq. (7), we find that there is no EGT term driving the zonal flow, only the FNP term. By comparing the diagnosed results and an analysis of the deriv-

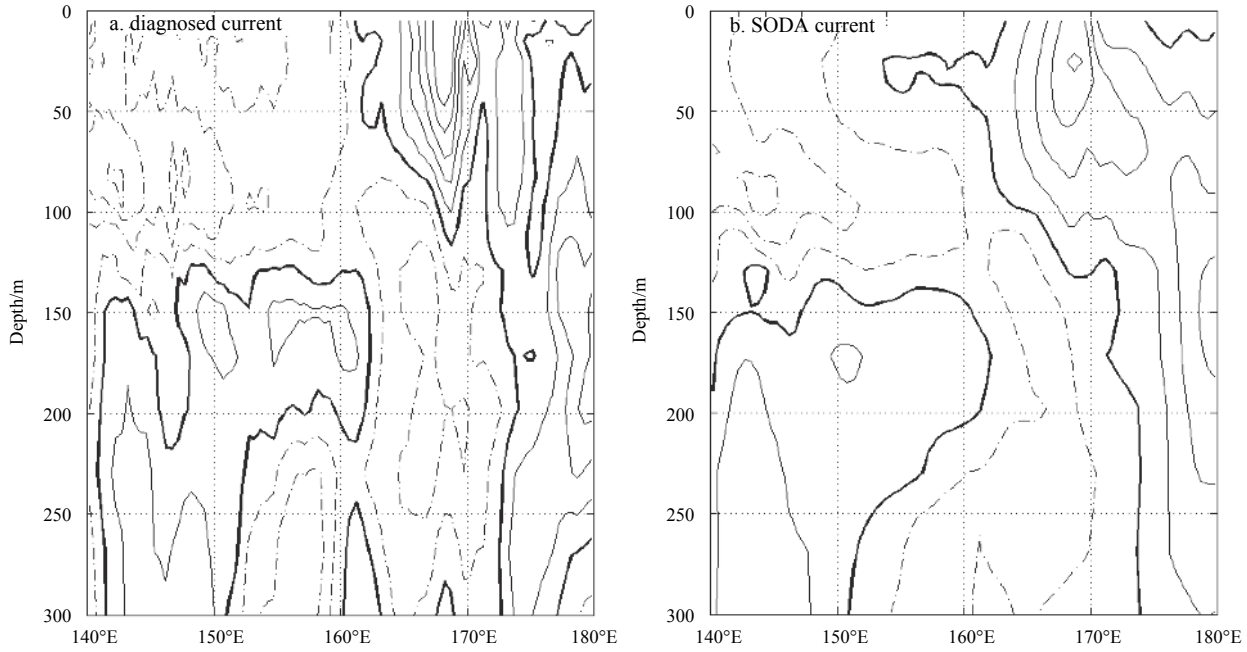

Fig. 4. Zonal velocity (m/s). a. Diagnosed result, and b. SODA_2.2.4_200001. $u < 0$ dashed contours, $u = 0$ thick solid contours, $u > 0$ solid contours; the contour interval is 0.2 m/s.

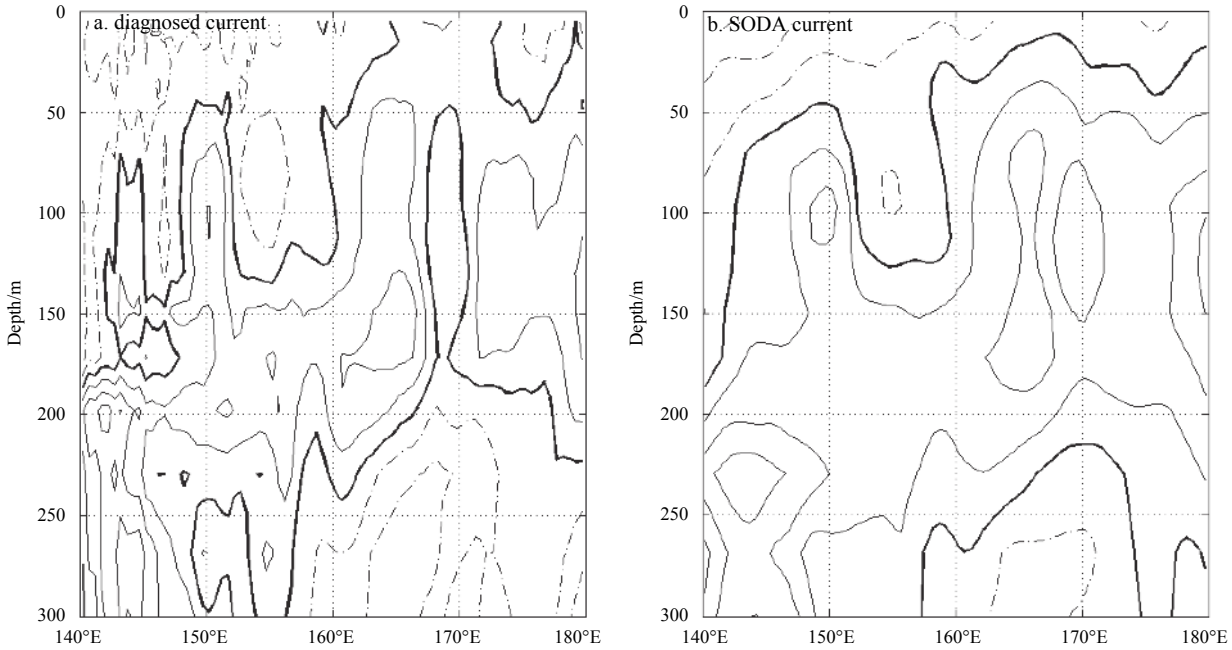

Fig. 5. Zonal velocity (m/s). a Diagnosed result, and b. SODA_2.2.4_200007. The contour lines are the same as in Fig. 4.

ing process, we find that the β-effect may be the main reason that the FNP is the only factor in Eq. (7).

From Eq. (7), a linear relationship between the FNP and the EUC can be written as

$$u = -\frac{a}{\rho\beta}\frac{\partial^2 p}{\partial y^2} + b, \tag{14}$$

where a and b are regression coefficients. This very simple relation gives us the relationship between the FNP (a function of pressure, temperature, salinity and density) and the EUC. Comparing $-\frac{1}{\rho\beta}\frac{\partial^2 p}{\partial y^2}$ with the velocities in the SODA, we find that this relation is $u = -\frac{1.02}{\rho\beta}\frac{\partial^2 p}{\partial y^2} + 0.06$ in all the data sets used in this study. In the area of eastward flow, the CCs and the regression coefficients for each grid point are presented in Fig. 7. Figure 7 shows that for the equatorial Pacific Ocean, the EUC is approximately equal to the FNP except in the western equatorial Pacific Ocean: west of about 143°E and below 150 m. The mean of the re-

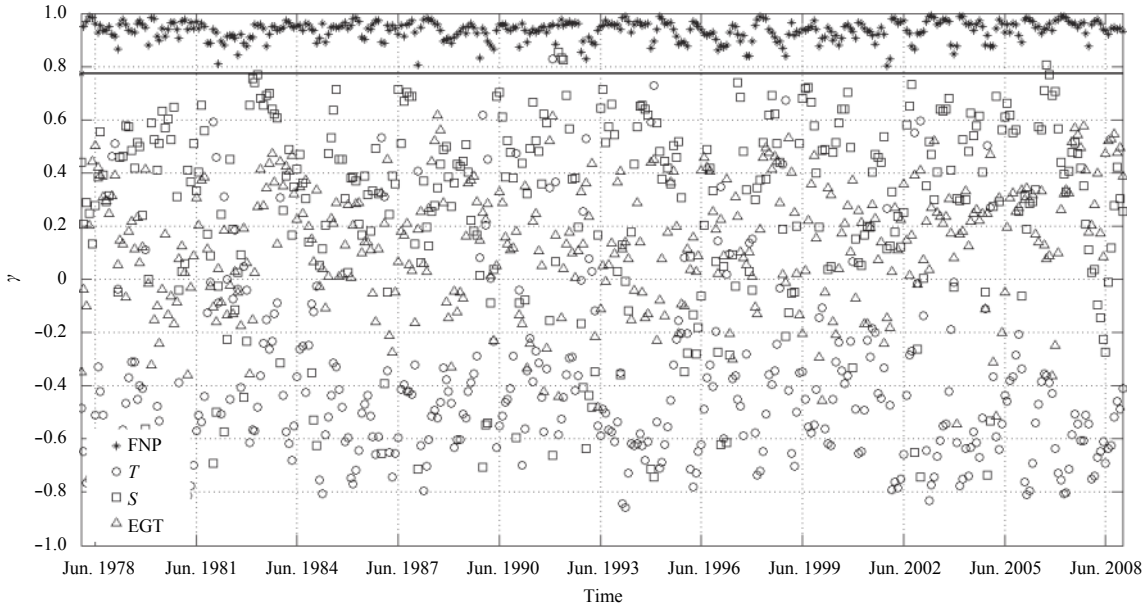

Fig. 6. CCs with respect to the EUC in the SODA. Asterisks indicate the CC for the diagnosed results, circles the CC for the temperature, squares for the salinity and triangles for the EGT. The solid line shows the minimum value of the CC for the diagnosed results.

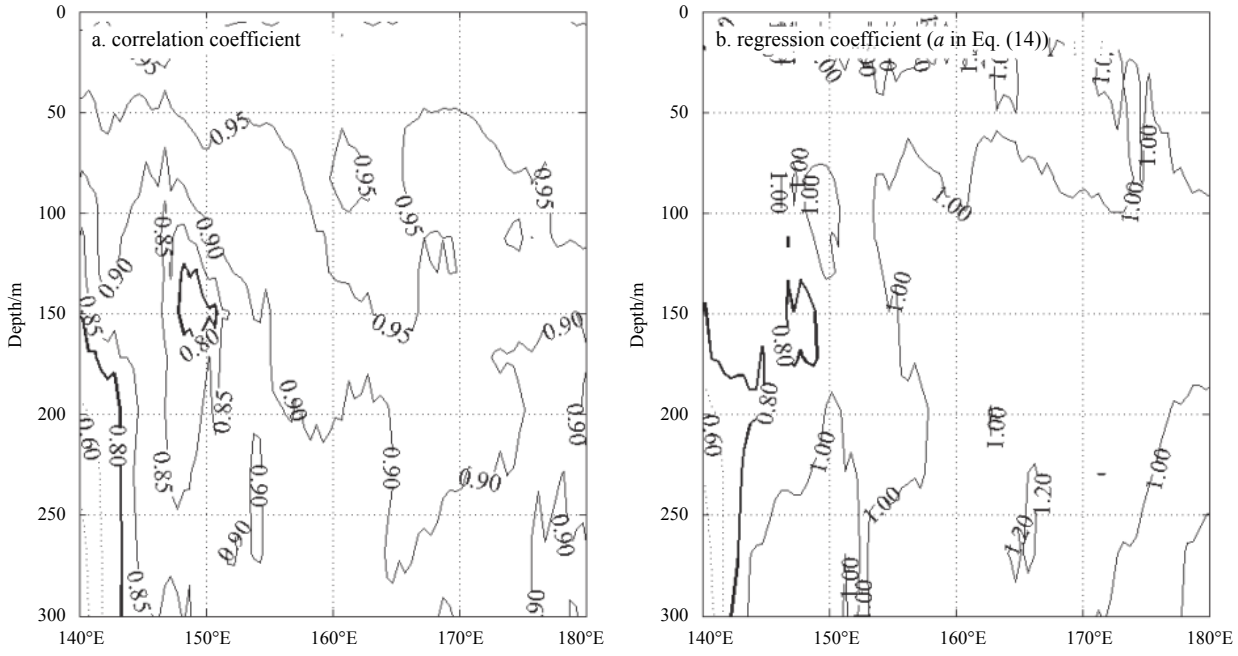

Fig. 7. Results of the comparison. a. The CC between the diagnosed results and the EUC in the SODA at each grid point, the CC is less than 0.8 dashed; b. the regression coefficient a in Eq. (14) in each grid, the regression coefficient a is less than 0.8 and greater than 1.2 dashed.

gression coefficient (b in Eq. (14)) is about 0.07, and the maximum absolute value of the regression coefficient (b in Eq. (14)) is less than 0.22. So, this relation is reliable.

4 Discussion and conclusions

Starting from the primitive equations, we have derived a relationship between the FNP and the EUC. With the numerical methods in Section 2, a method has been developed calculating the EUC. The results show that the FNP is closely associated with the EUC.

In essence, the relationship (Eq. (7)) is a balance between the pressure and the EUC. The FNP is not independent of other processes; the pressure is a linear integral function of density, but the density is a very complex nonlinear function of pressure (or depth approximately), sea temperature, and salinity. Many studies have considered the relationships between the sea surface height, the thermocline, the wind stress and other factors, such as the balance between a zonal wind stress and a depth-integ-

rated zonal pressure gradient (Yu and McPhaden, 1999), and the relationship between the wind stress and the EUC (Constantin and Johnson, 2015). For the equations controlling equatorial motion, the Coriolis force is replaced by βy (Hughes, 1981), and the zonal geostrophic balance was given as $u = -\frac{1}{\beta y}\frac{\partial(p/\rho)}{\partial y}$. But this function is an approximation to the relationship between the NGT and the EUC.

Figures 6 and 7 show that the FNP is highly correlated with the EUC, which indicates that the meridional differences of the temperature and the salinity are very important to the EUC. The FNP not only has an important influence on the EUC, but is also a response to the meridional difference of the primary factors (temperature, salinity, density and pressure). The distributions of the primary factor are influenced by the wind stress, solar radiation, and evaporation; all these meridional property differences have an impact on the EUC.

The relationship between the FNP and the EUC shows that the FNP may be more important than the EGT or other atmosphere-ocean factors to the EUC, as the FNP includes information on the temperature, the salinity, the thermocline, the depth and other factors that may be the density and the pressure. The FNP also represents the meridional differences of the temperature and the salinity, as the density and the pressure are calculated from both these properties. Because the FNP also includes information from the zonal differences of the temperature and the salinity, this relationship can also be used to study how the thermocline affects the EUC even when tendency terms are included.

Acknowledgements

Thanks for the support from Chen Nuo.

References

Brandt P, Funk A, Tantet A, et al. 2014. The Equatorial Undercurrent in the central Atlantic and its relation to tropical Atlantic variability. Climate Dynamics, 43(11): 2985–2997

Carton J A, Giese B S. 2010. A reanalysis of ocean climate using simple ocean data assimilation (SODA). Monthly Weather Review, 136(8): 2999–3017

Chen Xuan, You Xiaobao, Zheng Chongwei. 2017. Instruction to Mathematic Structures of Ekman Current. Saarbrücken: LAP LAMBERT Academic Publishing

Constantin A, Johnson R S. 2015. The dynamics of waves interacting with the Equatorial Undercurrent. Geophysical and Astrophysical Fluid Dynamics, 109(4): 311–358

Crawford W R. 1982. Pacific equatorial turbulence. Journal of Physical Oceanography, 12(10): 1137–1149

Drenkard E J, Karnauskas K B. 2014. Strengthening of the Pacific Equatorial Undercurrent in the SODA reanalysis: mechanisms, ocean dynamics, and implications. Journal of Climate, 27(6): 2405–2416

Hazeleger W, De Vries P, Friocourt Y. 2003. Sources of the Equatorial Undercurrent in the Atlantic in a high-resolution ocean model. Journal of Physical Oceanography, 33(4): 677–693

Holmes R M, Thomas L N. 2015. The modulation of equatorial turbulence by tropical instability waves in a regional ocean model. Journal of Physical Oceanography, 45(4): 1155–1173

Hughes L R. 1981. On inertial instability of the Equatorial Undercurrent. Tellus, 33(3): 291–300

Izumo T. 2005. The Equatorial Undercurrent, meridional overturning circulation, and their roles in mass and heat exchanges during El Niño events in the tropical Pacific ocean. Ocean Dynamics, 55(2): 110–123

Johns W E, Brandt P, Bourlès B, et al. 2014. Zonal structure and seasonal variability of the Atlantic Equatorial Undercurrent. Climate Dynamics, 43(11): 3047–3069

Kessler W S. 2006. The circulation of the eastern tropical Pacific: a review. Progress in Oceanography, 69(2–4): 181–217

Pedlosky J. 1987. An inertial theory of the Equatorial Undercurrent. Journal of Physical Oceanography, 17(11): 1978–1985

Pedlosky J, Samelson R M. 1989. Wind forcing and the zonal structure of the Equatorial Undercurrent. Journal of Physical Oceanography, 19(9): 1244–1254

Pham H T, Sarakar S, Winters K B. 2013. Large-eddy simulation of deep-cycle turbulence in an Equatorial Undercurrent model. Journal of Physical Oceanography, 43(11): 2490–2502

Qiu Bo, Chen Shuiming, Sasaki H. 2013. Generation of the north Equatorial Undercurrent jets by triad baroclinic rossby wave interactions. Journal of Physical Oceanography, 43(12): 2682–2698

Stewart R H. 2008. Introduction to Physical Oceanography. Florida: Orange Grove Texts Plus

Sudre J, Morrow R A. 2008. Global surface currents: a high-resolution product for investigating ocean dynamics. Ocean Dynamics, 58(2): 101–118

Sun Jilin, Chu P, Liu Qinyu. 2004. The seasonal variation of undercurrent and temperature in the equatorial Pacific jointly derived from buoy measurement and assimilation analysis. Acta Oceanologica Sinica, 23(1): 51–60

Swapna P, Krishnan R. 2008. Equatorial Undercurrents associated with Indian Ocean dipole events during contrasting summer monsoons. Geophysical Research Letters, 35(14): L14S04

Wang Hongna, Chen Jinnian, He Yijun. 2009. Variations of Equatorial Undercurrent and its relationship with ENSO cycle. Haiyang Xuebao (in Chinese), 31(3): 1–11

Wang Zongshan, Jin Meibing, Zou Emei, et al. 1993. The inversion of the Equatorial Undercurrent in the western tropical Pacific during 1986/1987 El Niño event. Acta Oceanologica Sinica, 12(4): 487–498

Wang Dailin, Müller P. 2002. Effects of Equatorial Undercurrent shear on upper-ocean mixing and internal waves. Journal of Physical Oceanography, 32(3): 1041–1057

Wang Fan, Wang Jianing, Guan Cong, et al. 2016. Mooring observations of equatorial currents in the upper 1000 m of the western Pacific Ocean during 2014. Journal of Geophysical Research: Oceans, 121(6): 3730–3740, doi: 10.1002/2015JC011510

Yin F L, Sarachik E S. 1993. Dynamics and heat balance of steady Equatorial Undercurrents. Journal of Physical Oceanography, 23(8): 1647–1669

Yu Xuri, McPhaden M J. 1999. Dynamical analysis of seasonal and interannual variability in the equatorial Pacific. Journal of Physical Oceanography, 29(9): 2350–2369

Zheng Chongwei, Li Chongyin. 2017. Propagation characteristic and intraseasonal oscillation of the swell energy of the Indian Ocean. Applied Energy, 197: 342–353

Zheng Chongwei, Li Chongyin, Pan Jing. 2018a. Propagation route and speed of swell in the Indian Ocean. Journal of Geophysical Research: Oceans, 123: doi: 10.1002/2016JC012585

Zheng Chongwei, Xiao Ziniu, Zhou Wen, et al. 2018b. 21st Century Maritime Silk Road: A peaceful way forward. Singapore: Springer Nature Singapore Pte Ltd